NASA Technical Memorandum 87234

NASA-TM-87234 19860012323

Effect of a Rotor Wake on the Local Heat Transfer on the Forward Half of a Circular Cylinder

Kim A. Morehouse and Robert J. Simoneau
Lewis Research Center
Cleveland, Ohio

March 1986

NASA

EFFECT OF A ROTOR WAKE ON THE LOCAL HEAT TRANSFER ON THE

FORWARD HALF OF A CIRCULAR CYLINDER

Kim A. Morehouse and Robert J. Simoneau
National Aeronautics and Space Administration
Lewis Research Center
Cleveland, Ohio 44135

SUMMARY

An experiment has been developed to simulate the wake dynamics of a turbine rotor-stator combination. The experiment consisted of a spoked wheel rotating in annular flow, generating simulated rotor wakes. The wakes impinged on a simulated stator, composed of a circular cylinder with a splitter plate behind it. The test rig properly simulated the wake shapes and velocity dynamics of a rotating turbine stage. The focus of the research was spanwise averaged circumferentially local heat transfer in the circular cylindrical leading edge region of a turbine airfoil. The range of Reynolds number based on the stator cylinder diameter was 35 000 to 175 000. The reduced blade passing frequencies, or Strouhal numbers, also based on the stator cylinder diameter, ranged from 0.63 to 2.50. The wakes were generated by two different sets of circular cylindrical bars, 1.59 and 3.18 mm in diameter. The rotor could be rotated either clockwise or counterclockwise, causing the wakes to impinge on either the leeward or the windward side of the heated cylinder. In addition, grid turbulence was introduced upstream yielding freestream turbulence of 1.0 to 2.5 percent at the stator location.

The data presented in this paper, therefore, represent an extensive body of local heat transfer coefficients, which can be used to develop models in the very important leading edge region of a turbine airfoil. The wakes produced only a modest increase in heat transfer over the baseline no-rotor data. The data in the presence of the rotor wakes showed an asymmetry from the leeward to the windward side. Windward side levels of from 30 to 40 percent higher than corresponding leeward-side levels were not uncommon, particularly at the combination of high Strouhal number and larger wake generating pins. The stagnation gauge data were examined against the $Tu\sqrt{Re}$ parameter over a wide range from 8 to 40, and found not to be fully correlated by this often used parameter. There were distinct trends with both free-stream turbulence level and wake-generating bar diameter. The results strongly indicate a need to separate the wake influence from turbulence effects.

INTRODUCTION

Considerable effort is being directed these days at heat transfer in unsteady flow fields. Probably among the oldest unsteady effects studied are those which occur naturally in the flow, such as one body in the wake of

---

another or the effect of natural instabilities. Another area involves oscillations of the entire flow field, such as might occur downstream of a pump. A third type of unsteadiness, the type of interest herein, is a forced, periodic and localized, disturbance of the flow, such as occurs where a moving object cuts across the flow path, as in a turbine.

Research on heat transfer in these flow fields is just beginning. Work includes heat transfer in turbines (refs. 1 to 4), as well as in the wakes of spoked wheel or squirrel cage disturbance generators (refs. 5 to 9). The exact nature of the moving wakes on heat transfer awaits more research; however, in general it can be said that these disturbances enhance heat transfer. The passing of the wakes can produce some dramatic local unsteady heat transfer effects, as shown by Doorly and Oldfield (ref. 6), Ashworth et al., (ref. 7). The effect on steady heat transfer, especially when combined with normal turbulence, is not uniformly clear, as shown by Dunn (refs. 1 to 3), for example.

There is a growing opinion which suggests that it will be necessary to sort out the periodic unsteadiness from the random turbulence. Jayaramon, Parikh, and Reynolds (ref. 10) propose a triple decomposition of the velocity vectors. Adamczyk (ref. 11) also recommends changes in turbomachinery closure modeling. The extend and detail of what must be done will be evolving for sometime.

The experiment reported herein simulated a turbine rotor wake with a rotating spoked wheel. The leading edge of the airfoil in the wake was simulated with a circular cylinder with a splitter plate behind it. Spanwise averaged, circumferentially local heat transfer was measured for angles from 0° to 79° from stagnation on both the windand leeward side relative to the convected wake. Reference data were acquired at various turbulence levels with the rotor removed. An attempt is made to sort out the two effects.

NOMENCLATURE

A   cross sectional area, m^2

A_s surface area, m^2

d   diamter, m

f   frequency, Hz

I   current, amps

k   thermal conductivity, $w/m^2 \cdot K$

m   mass flux, kg/m^2 sec

Nu   Nusselt number, dimensionless

Pr   Prandtl number, dimensionless

Q   heat, power, w

Re   Reynolds number, dimensionless

S   Strouhal number, dimensionless

T   temperature, K

Tu   unsteadiness parameter, dimensionless

$\bar{u}$ average velocity, m/sec

u' fluctuating velocity, m/sec

V   voltage, volts

μ viscosity, N-sec/m^2

Subscripts:

avg   average

aw   adiabatic wall

ref   reference

o   stagnation condition

s   static condition

w   wall condition

ROTOR WAKE SIMULATION

The simulation employed in this experiment is illustrated in figure 1.
In part (a) a typical turbine stage with the wake-related velocity triangles
is shown. Only two points are important. First, whether one is looking at
the rotor passing into a stator wake or a rotor wake being carried into a sta-
tor passage, the effect is the same. The suction surface sees the wake first
and the change in incidence is towards negative incidence. The simulation
produced by a circular rod passing across the flow field is shown in part (b).
The major features are clearly the same.

The simulation used in the present experiment is illustrated in figure 2.
A spoked wheel rotates in an annular flow passage producing the desired wakes.
Since the focus is on the leading edge region, the downstream airfoil is even
further simplified by using a circular cylinder with a splitter plate behind
it to eliminate alternate shedding vortices.

Typical instantaneous and ensemble-averaged wakes produced in the simula-
tion rig (more information on them appears in ref. 5) are shown in figure 3.
The combination of the turbulence and the periodic unsteadiness is apparent
in figure 3(a). The random components disappear in the averaging process,
figure 3(b). These wakes were compared to compressor wakes measured by Evans
(ref. 12) and found to exhibit all the major features of depth, width and so
on.

DESCRIPTION OF EXPERIMENT

The key element in the present experiment is the segmented copper heat transfer cylinder, shown in figure 4. The test section was a 2.62 cm diameter circular cylinder composed of 15 individually controlled heater elements, which served as heat transfer gauges. Each heater was made of a solid copper bar with a thermocouple (Type E) buried near the surface and a heater element at the back. The temperature signal from each element was fed into an electronic control circuit, described in reference 13, which controlled the power to each heater such that the temperature of all elements was held constant to within 0.1 K. Thus, the experiment is an isothermal wall boundary condition. Twelve of the heater elements were spaced around the cylinder circumference at nominally 11° increments, as can be seen in figure 4. The two end elements served as guard heaters, leaving 10 active heat transfer elements. Both of the spanwise ends had a guard heater, as shown. The back of the whole assembly was also guarded. This element, of course, cannot be seen in the photograph. Each of the active heat transfer elements was 2.50 mm wide by 33.0 mm long. Each element had a mylar and epoxy insulating space between them. It can be seen from the photograph that the installation was not perfectly equispaced. (It must be remembered that all 15 elements with heater lead wires and thermo couples for each were stuffed into a package only 2.62 cm in. diam.) The actual center-to-center spacing was measured and these actual angles are used in the data reporting. The photograph, figure 4, was taken after the experiment and shows a small nick in one of the heaters. This occurred midway through the experiment, when the smaller pins broke. It appeared to have no effect on the subsequent data.

The circumferentially segmented heated test cylinder was installed in the rotor-wake rig, shown in figure 5, at a distance 2.5 cm downstream of the spoked rotor. Thus, the wakes were being generated one stator diameter upstream of the stator stagnation line. The flow facility and its characteristics are described in some detail in reference 5. Only those details essential to the present experiment will be described herein. The flow facility was at room temperature and pressure annular flow wind tunnel. The flow annulus was 40.6 cm o.d. by 27.1 cm i.d., providing a 0.722 m^2 flow cross section. The heated cylinder was one of eight stators equispaced circumferentially around the annulus, each with a 1.6 mm thick splitter plate behind, as illustrated in figure 2. The heated stators provided a 20 percent flow blockage. The wake generating rotor was a spoked wheel of 24 cylindrical pins, as illustrated in figure 2. There were two pin diameters, 1.59 mm and 3.18 mm. The rotor was driven with a motor and pulley arrangement. It could be driven both forward and reverse and could be controlled at speeds from 500 to 7300 rpm. The turbulence was controlled with square pattern woven wire screens with approximately two-thirds open area. Two grid sizes, 10-mesh and 3-mesh, were used. (The x-mesh terminology is an American wire manufacturer designation standing for x wires per inch and does not translate well to SI units. For convenience this jargon will be used herein.) The 3-mesh grid had 1.6 mm wires spaced about 8.5 mm apart and the 10-mesh grid had 0.25 mm wires spaced about 2.5 mm apart. Except for one dataset the grids were located 21.0 cm upstream of the stator leading edge. (In one case the 3-mesh grid was located 10.8 cm upstream.)

As indicated above, the heat transfer from each element was determined by measuring the power delivered to each individual backside heater and the temperature of the copper element with a thermocouple buried in it. The tunnel

mass flow rate was measured with a sharp edged orificed designed to ASME standards. This measurement was backed up by treating the inlet contraction as on isentropic nozzle. Velocity was measured at two locations, one half way between the turbulence grid and the stator plane and the other at the stator stagnation plane, using a pilot-static probe. Velocities and turbulence intensities were also measured at the same locations with single-wire hot wire anenometers. The rotor speed was measured with a fiber optic probe sighted on the tip of one of the rotor pins painted white. This was backed up by a 60-tooth gear and magnetic pickup on the rotor drive shaft.

The data are presented in terms of Nusselt, Reynolds and Strouhal numbers and also an unsteadiness or turbulence parameter, all defined below.

The Reynolds number is based on a mass-averaged velocity and free-stream properties.

$$Re = \frac{md}{A\mu}$$

The Strouhal or reduced frequency is based on the rotor circular frequency and the same mass-averaged velocity. Expressed in terms of the rotor pin (blade) passing frequency it is:

$$S = \frac{2\pi fd}{\bar{u}}$$

The Nusselt number is defined in the following manner.

$$Nu = \frac{(Q_{tot} - Q_{loss})\, d}{(T_w - T_{aw})\, A_s k}$$

The total heat flux is based on the total power dissipated, VI. The heat loss correction has two components; the radiation loss, which was usually quite small, and the loss through the insulating strips, which was occasionally large and varied from strip to strip. The insulation loss was determined analytically, based on a model presented in reference 13. The adiabatic wall temperature assumed a laminar flow Prandtl number relationship

$$T_{aw} = T_0 - \sqrt{Pr}\, (T_0 - T_s)$$

and the thermal conductivity was calculated on the basis of the Eckert (ref. 14) reference temperature

$$T_{ref} = 0.50\, T_w\Big)_{avg} + 0.28\, T_s + 0.22\, T_{aw}$$

Finally, an unsteadiness parameter is defined as

$$Tu' = \frac{u'_{rms}}{\bar{u}}$$

5

The unsteadiness is simply the root-mean-square of the velocity flucations divided by the integrated time average of the velocity, as measured by the hot wires. In the absence of the rotor wakes it is the familiar turbulence intensity, Tu. In the wake of the rotor it includes both the random turbulence and the periodic unsteadiness of the wakes, as shown in figure 3.

An uncertainty analysis, based on the method of Kline and McClintok (ref. 15), was included in the data reduction program and every dataset included uncertainty estimates. These will be shown on the results figures, as appropriate. While the uncertainty varied from run to run, and in the case of Nusselt number from heater strip to heater strip, the average values were: Nusselt number 6 percent, Reynolds number 1 percent, Strouhal number 1 percent, and unsteadiness parameter 1 percent.

Finally, before initiating the experiment, flow angle measurements were made behind the rotor. An example for the 1.59 mm pins is available in reference 5. For both pin sizes the combinations of Reynolds and Strouhal selected were such that the flow angle was always less than 3°.

RESULTS

No Rotor Reference Cases

In order to establish a reference database, and to compare existing data to the literature a series of cases were run with the spoked rotor removed. In the first case the heated cylinder was rotated to various angular positions, causing different elements to be the stagnation gauge, in order to see if there was any gauge bias. The results, shown in figure 6, show very little sensitivity to gauge position except for one case at the lowest Reynolds number. The variation from gauge to gauge was well within the average uncertainty band of the stagnation gauge, which is included on the figure. One will note that, except at the stagnation point, the data do not line up with the angles. This is because, as explained earlier, the gauges are not spaced at equal angles; and, when the cylinder is rotated, the angle relative to stagnation changes. There appears to be a slight dip in heat transfer in the stagnation region. Since the dip is within the uncertainty band, one must be cautious in drawing conclusions. However, the dip appears to be independent of gauge selection and has been observed by others (ref. 16).

In order to obtain data over a large angle range (0° to 79°) gauge 8 was selected to be the stagnation gauge. It was selected over number three, because the uncertainty was always lower. With this choice all the remaining data were acquired with gauge 8 on the stagnation line. This left two active gauges to the opposite side as a check. In the following figures only the eight gauges to one side of stagnation will be shown to avoid confusion.

The no rotor data over the full Reynolds number range of the experiment are shown in figure 7. The error band for each gauge is shown for one of the Reynolds numbers, as typical. The data represent two turbulence levels, approximately 1 percent and 2 percent. For each level, higher Reynolds numbers yielded slightly lower turbulence intensity. The doubling of turbulence intensity from 1 to 2 percent leads to a 5 to 10 percent increase in heat transfer, this increase being greater at the higher Reynolds number. The increase is

6

pretty uniform for all angles. These data form a baseline reference for the rotor-wake cases.

Despite the large body of data on heat transfer to cylinders in crossflow, when one wishes to make comparisons, it is difficult to find datasets which matchup all conditions. For comparison to the present data the experiments of Kestin and Wood (ref. 17), VanFossen (ref. 18) and Giedt (ref. 18) were used. The comparisons are shown in figure 8, for Reynolds numbers in the range of 95 000 to 100 000. A third dataset, with higher turbulence level, was added to the data already shown on figure 7 for Re = 97 200. These data were obtained with the 3-mesh grid only 10.8 cm from the heater cylinder, as was mentioned above. Although the data of Kestin and Wood (ref. 17) were actually mass transfer sublimation data, the flow conditions most closely match the present data. The comparison is quite good except at the large angles. The data of Van Fossen (ref. 18) agree very well but his data only go out to 50°. The turbulence for these data were generated with parallel wires rather than a square mesh grid. The comparison with Giedt (ref. 19) is less satisfactory both in level and angular dropoff. Giedt's data were uniform heat flux rather than uniform temperature. Papell (ref. 20) showed that uniform heat flux data dropoff more slowly than uniform temperature, which could explain the observed angle variation. The level, especially at stagnation is harder to explain, except that Giedt estimated his turbulence intensity, while all the others measured it. In general, within experimental uncertainty, the present data agree well with the literature, well enough at least to draw valid comparisons between the no-rotor and rotor-wake data in the same experiment.

Rotor Wake Data

A very extensive dataset was acquired in the present experiment, more than can be presented herein. A selected subset is shown in figure 9(a) to (d). Two midrange Reynolds numbers and all three Strouhal numbers are presented. Each plot is for a different combination of pin diameter and turbulence grid, four in all. In addition, each plot includes data from wakes produced by both forward and reversed motion of the spoked rotor. A small diagram of the geometry of the flow field is shown on each plot. For the data to the left of center the wake is convected in at the heat transfer gauges (i.e., the windward side) and to the right of center the gauges are in the shadow of the convected wake (i.e., the leeward side). Recall, the wake flow angles are always less than 3°. In terms of the simulation the left hand (windward) data would represent the suction surface of a turbine airfoil and the right hand (leeward) the pressure surface.

Examining figures 9(a) to (d), one is struck by the strong similarity from case to case. The effects of Strouhal number are small but systematic. Although the effects are on the same order of the uncertainty bands, the fact that they are so consistently systematic is probably relavant. There is a definite asymmetry in the data, especially at the higher Strouhal numbers and with the larger pins.

In order to get a better appreciation for the various effects, a cross plot of the data was used. The data for one Reynolds number (125 400) and one Strouhal number (1.27) are plotted for all four pins and grid combinations. In addition the no-rotor data are plotted, including the highest turbulence (grid at 10.8 cm) case. To aid in comparison the no-rotor data are plotted to

both the right and left of zero on figure 10. They are not two datasets.
Thus, gauge 7 data appears at ±10°, gauge 6 data at ±25°, and so on. The
average uncertainty band for the stagnation gauge is shown on the figure.
Many of the observations to be made fall within this band.

First, let us focus on the data associated with the 10-mesh grid. In
the stagnation region the rotor-wake data show a very modest (6 to 7 percent)
increase in heat transfer, which is within the uncertainty. In fact, the
small-pin data are higher than the large-pin, which does not seem right.
Nevertheless, the data are higher. On the leeward side these modest increases
persist over the whole angle range. On the windward side, as the flow pro-
gresses to higher angles, a more substantial wake-induced increase in heat
transfer occurs, reaching almost 50 percent over the no-rotor data at 79°.
This is, of course, near separation. However, except at the 79° point, all
of the 10-mesh data fall below the no-rotor 3-mesh data sets. This, despite
the fact that the wake related turbulence/unsteadiness rms is approximately
5 percent for the 1.59 mm pins and 9 percent for the 3.18 mm pins. In fact,
an almost doubling of the rms unsteadiness seems to have almost no effect on
average heat transfer. This important result points out the danger of treating
the wake-induced unsteadiness as a simple turbulence intensity.

The insertion of the 3-mesh grid at the 21.0 cm upstream location produced
about a 70 percent increase in the baseline turbulence. This increase shifted
all of the spanwise-averaged heat transfer data, both no-rotor and rotor wake,
up uniformly, about 13 percent at stagnation. Curiously, increasing the base-
line turbulence appears to have little or no effect on the rms turbulence/
unsteadiness of the rotor wakes, but it does affect the heat transfer. Finally,
one notes that increasing the grid turbulence to a modest level of 2.84 percent
produces a higher heat transfer level than all the rest of the heat transfer
data.

It has become common to express cylinder in crossflow heat transfer data
as $Nu/\sqrt{Re}$ verses $Tu\sqrt{Re}$. Kestin and Wood (ref. 17) and Lowery and Vachon
(ref. 21) proposed quadratic correlations for the stagnation line heat transfer
which are often used. Lowery and Vachon (ref. 21) also showed that the same
trends as at stagnation existed for overall heat transfer, but, of course, at
lower average values. In reference 5 the present authors suggested that over-
all heat transfer to a circular cylinder in the wake of a spoked rotor could
be correlated in the same manner by treating the rms flucuations behind the
rotor as turbulence. Following up on that suggestion, the stagnation gauge
data for all cases are shown in these variables on figure 11 along with the
data of Lowery and Vachon. The no rotor data agree well with data of Lowery
and Vachon. The rotor-wake data do not agree and they do not correlate in
these variables. This is not too surprising in light of the previous figure.
What was thought to be a correlating trend in reference 5, was not. The dif-
ference in the present experimental conditions from the previous is the addi-
tion of 3.18 mm pins. They were not used in reference 5. Since the larger
pins double the rms flucuations but make very little effect on the heat trans-
fer, Tu' cannot be a correlating parameter. Actually, if one were to ignore
the wake and use the grid turbulence level, the data would probably fall within
the wide band of the no rotor data, shown in figure 11. This representation
would be wrong, however, since the wakes do have an effect on stagnation heat
transfer, albeit small.

The main effect of the wakes on the spanwise average heat transfer is the angular asymmetry. This effect is best shown in figure 12, where the ratio of windward-to-leeward heat transfer is plotted against angle from stagnation for the data of figure 9. There is quite a bit of scatter in this data, nevertheless clear trends do exist. Lines were drawn roughly through the data to aid in interpretation. In this representation it can be seen clearly that pin size and Strouhal number (rotor speed) make a difference. There appeared to be no special influence of grid turbulence or Reynolds number on this asymmetry. Although there is a definite trend at all angles, at angles below about 40° the asymmetry was less than 5 percent, which is within the uncertainty. At the lowest Strouhal number, 0.62, the asymmetry ranged from 5 percent with the small pins to 10 percent with the large pins. At the highest Strouhal number, 2.51, the asymmetry range was 35 to 50 percent at the higher angles. It should be noted that on an airfoil the circular leading edge is faired smoothly to the rest of the airfoil and thus separation effects are minimized. The large effects seen herein at large angles should not be present on an airfoil but the asymmetry will be present. Further investigation on airfoils is warranted.

CONCLUSIONS

An experiment was performed in which the wake effects of a turbine stage were simulated using a spoked-wheel rotor and downstream circular cylinder as a stator leading edge. Spanwise average circumferentially local heat transfer coefficients were measured over a range of Reynolds and Strouhal numbers and at two levels of grid-generated turbulence. The rotor could be rotated in either direction, resulting in the wakes being convected both into and away from the heated surface. The primary conclusions from this experiment are as follows:

1. The wakes induced by the spoked rotor produce a modest increase in heat transfer over the no-rotor reference case.

2. Increasing the baseline turbulence shifts both the no rotor reference case and the rotor-wake heat transfer data up uniformly.

3. The wake-generated rms unsteadiness is not a correlating parameter and should not be classified as turbulence. The data strongly support the need to separate out the effects of random turbulence and periodic unsteadiness and treat them separately.

4. The convected wakes produce a significant asymmetry in heat transfer around the leading edge of the heated cylinder from the side impacted by the wakes to the side shielded from the wakes. This asymmetry increases with Strouhal number and wake size.

REFERENCES

1. Dunn, M.G.; Rae, W.J.; and Holt, J.L.: Measurement and Analysis of Heat Flux Data in a Turbine Stage: Part I - Description of Experimental Apparatus and Data Analysis. J. Eng. Gas Turbines Power, vol. 106, no. 1, Jan. 1984, pp. 229-233.

2. Dunn, M.G.; Rae, W.J.; and Holt, J.L.: Measurement and Analysis of Heat Flux Data in a Turbine Stage: Part II - Discussion of Results and Comparison with Predictions. J. Eng. Gas Turbines Power, vol. 106, no. 1, Jan. 1984, pp. 234-240.

3. Dunn, M.G.: Detailed Heat-Flux Measurements for the Blade Surface in a Full-Stage Rotating Turbine. Paper submitted to ASME 31st Inter. Gas Turbine Conf., Dusseldorf, W. Germany, June 1986.

4. Dring, R.P., et al.: Turbine Rotor-Stator Interaction. J. Eng. Power, vol. 104, no. 4, Oct. 1982, pp. 729-742.

5. Simoneau, R.J.; Morehouse, K.A.; and VanFossen, G.J.: Effect of a Rotor Wake on Heat Transfer from a Circular Cylinder. ASME Paper 84-HT-25, Aug. 1984.

6. Doorly, D.J.; and Oldfield, M.L.G.: Simulation of the Effects of Shock Wave Passing on a Turbine Rotor Blade. ASME Paper 85-GT-112, Mar. 1985.

7. Ashworth, D.A., et al.: Unsteady Aerodynamic and Heat Transfer Processes in a Transonic Turbine Stage. ASME Paper 85-GT-128, Mar. 1985.

8. Bayley, F.J.; and Priddy, W.J.: Effects of Free-Stream Turbulence Intensity and Frequency on Heat Transfer to Turbine Blading. J. Eng. Power, vol. 103, no. 1, Jan. 1981, pp. 60-64.

9. Pfeil, H.; Herbst, R.; and Schroder, T.: Investigation of the Laminar-Turbulent Transistion of Boundary Layers Disturbed by Wakes. J. Eng. Power, vol. 105, no. 1, Jan. 1983, pp. 130-137.

10. Jayaramon, R.; Parikh, P.; and Reynolds, W.C.: An Experimental Study of the Dynamics of an Unsteady Turbulent Boundary Layer. (TF-18, Stanford Univ.; NASA Contracts ARO-1-80;-2-81;-1-82) NASA CR-170278, 1982.

11. Adamczyk, J.J.: A Model Equation for Simulating Flows in Multistage Turbomachinery. ASME Paper 85-GT-226, Mar. 1985.

12. Evans, R.L.: Turbulence and Unsteadiness Measurements Downstream of a Moving Blade Row. J. Eng. Power, vol. 97, no. 1, Jan. 1975, pp. 131-139.

13. VanFossen, G.J., et al.: Heat Transfer Distributions Around Nominal Ice Accretion Shapes Formed on a Cylinder in the NASA Lewis Icing Research Tunnel. AIAA Paper 84-0017, Jan. 1984.

14. Eckert, E.R.G.; and Drake, R.M.: Heat and Mass Transfer, 2nd ed., McGraw Hill, New York, 1959.

15. Kline, S.J.; and McClintock, F.A.: Describing Uncertainties in Single-Sample Experiments. Mech. Eng., vol. 75, no. 1, Jan. 1953, pp. 3-8.

16. O'Brien, J.E.; and VanFossen, G.J., Jr.: The Influence of Jet-Grid Turbulence on Heat Transfer from the Stagnation Region of a Cylinder in Crossflow. ASME Paper 85-HT-58. Aug. 1985.

17. Kestin, J., and Wood, R.T.: The Influence of Turbulence on Mass Transfer from Cylinders. J. Heat Trans., vol. 93, no. 4, Nov. 1971, pp. 321-327.

18. Van Fossen, G.J.: - private communication.

19. Giedt, W.H.: Effect of Turbulence Level of Incident Air Stream on Local Heat Transfer and Skin Friction on a Cylinder. J. Aeronaut. Sci., vol. 18, no. 11, Nov. 1951, pp. 725-730.

20. Papell, S.S.: Influence of Thermal Boundary Conditions on Heat Transfer from a Cylinder in Crossflow. NASA TP-1894, 1981.

21. Lowery, G.W.; and Vachon, R.I.: The Effect of Turbulence on Heat Transfer from Heated Cylinders. Int. J. Heat Mass Trans., vol. 18, no. 11, Nov. 1975, pp. 1229-1242.

(a) Turbine stage.
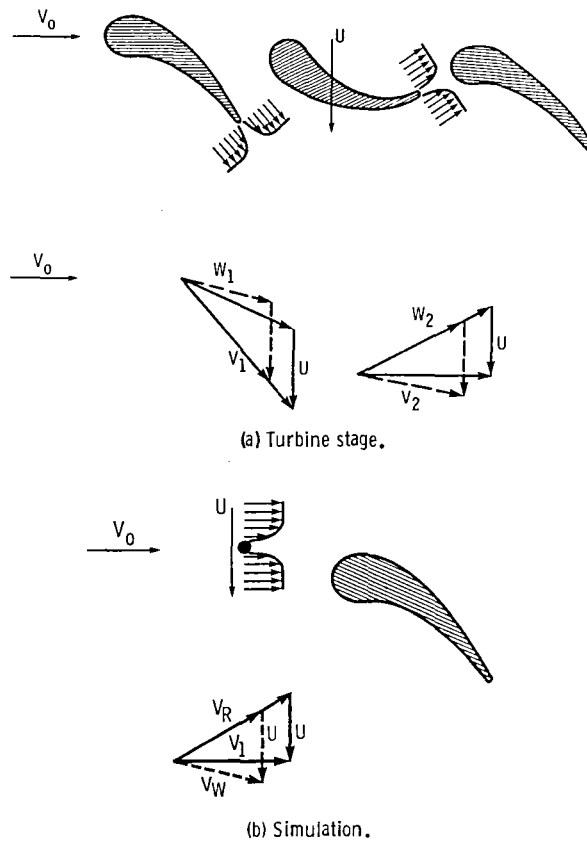
(b) Simulation.

Figure 1. - Simulation of turbine wakes using a spoked wheel disturbance generator.
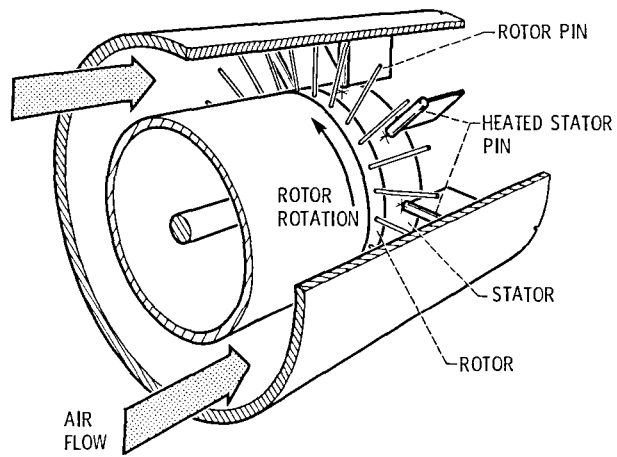
Figure 2. - Concept of rotor wake heat transfer experiment.
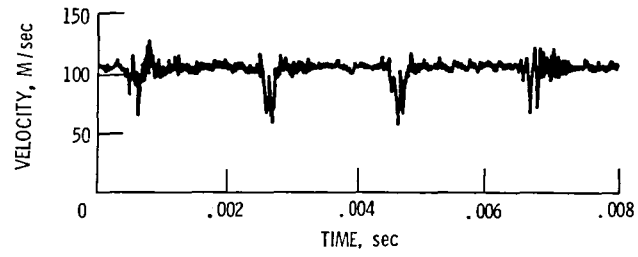
(a) Instantaneous wake.
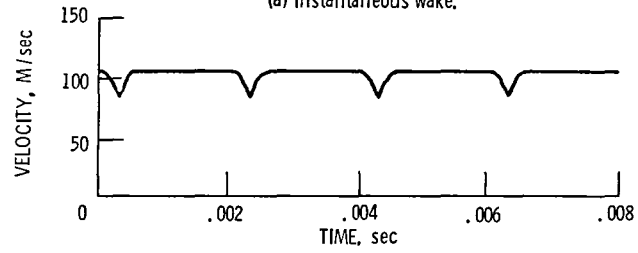
(b) Ensemble averaged wake.

Figure 3. - Typical wakes generated by a spoked wheel disturbance generator.
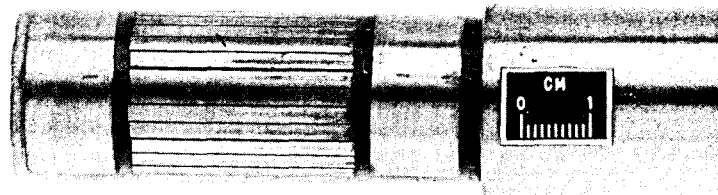
C-84-0797

Figure 4. - Photograph of circumferentially segmented copper heater.
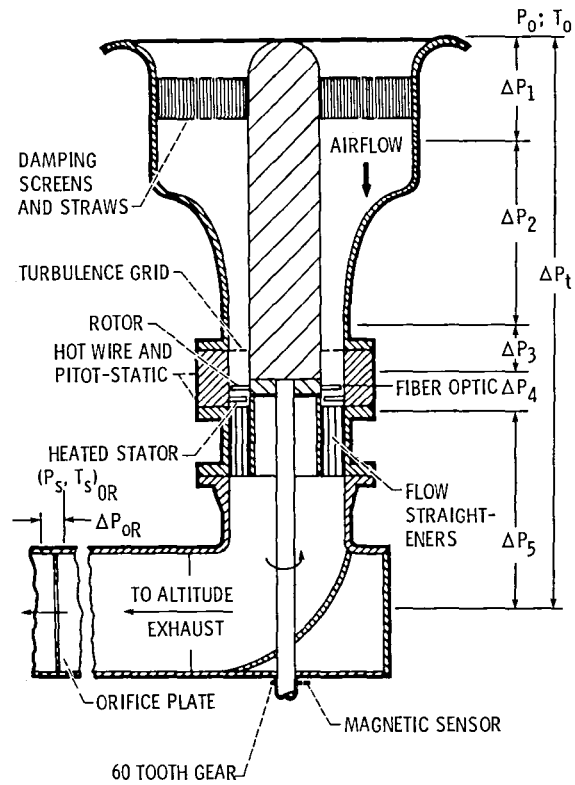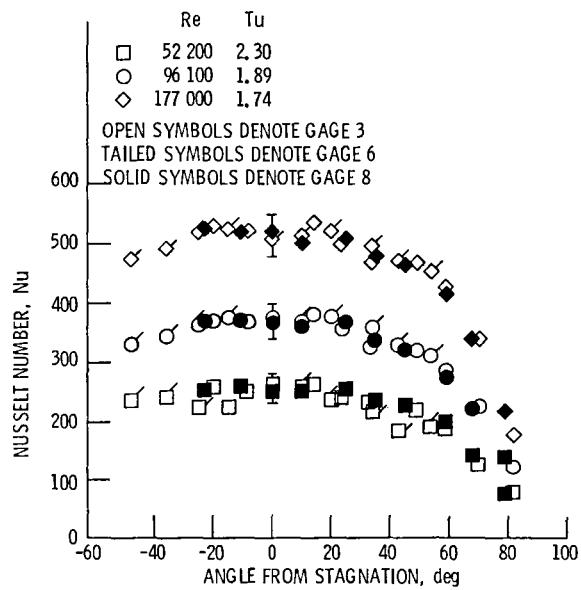
Figure 5. - Rig flow schematic.

Figure 6. - Effect of circumferential position of stagnation gage on Nusselt number distribution.
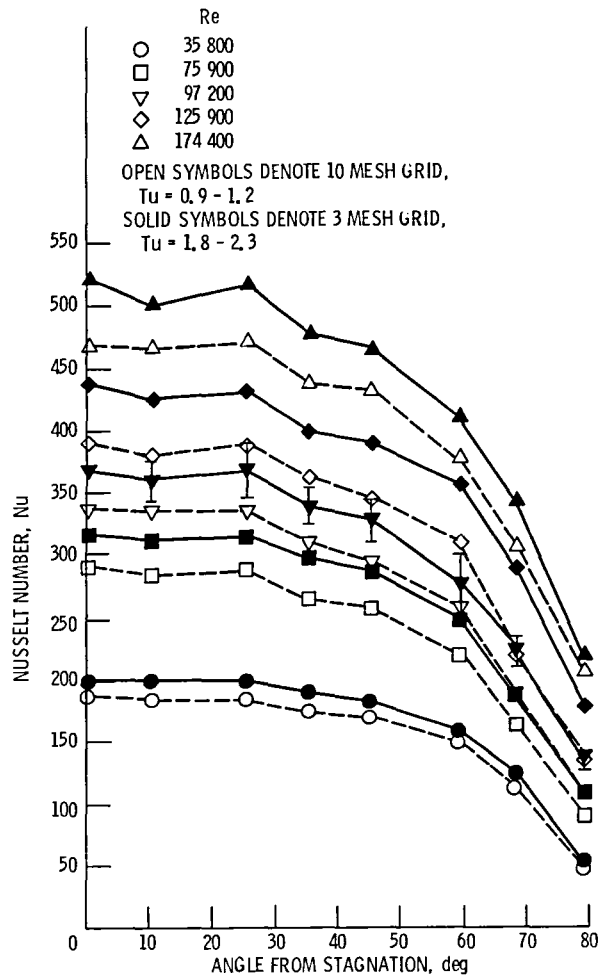
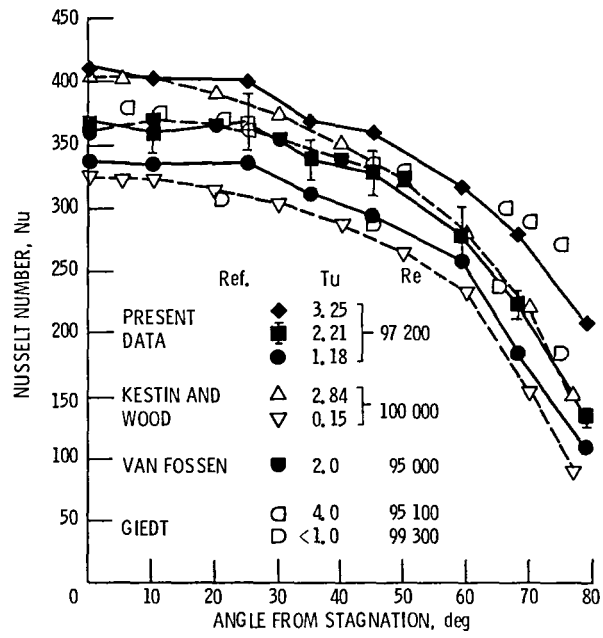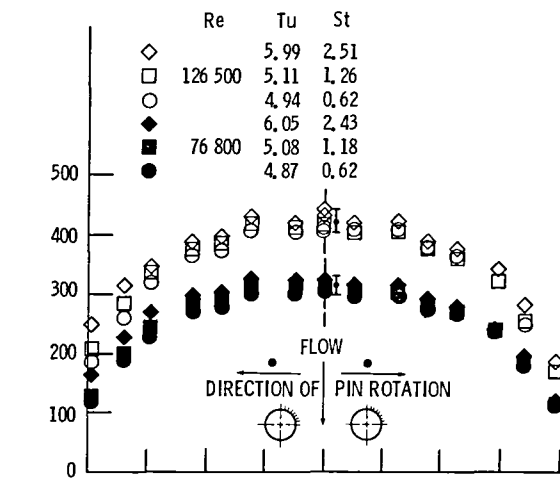Figure 7. - Spanwise average circumferential Nusselt number distribution as a function of Reynolds number and turbulence level with the rotor removed.
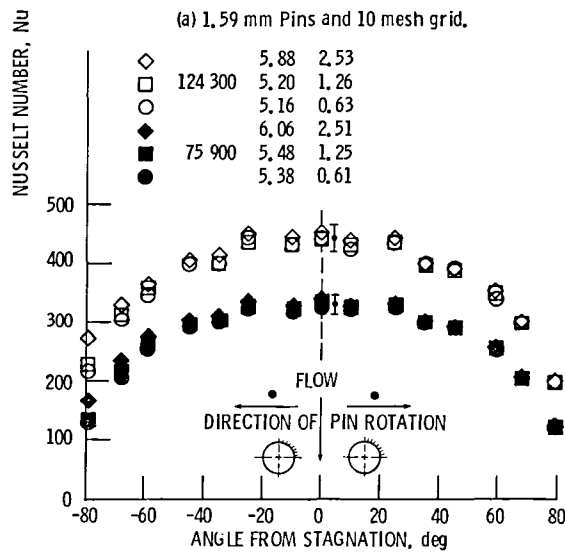
Figure 8. - Comparison of present data (rotor removed) with other experiments.
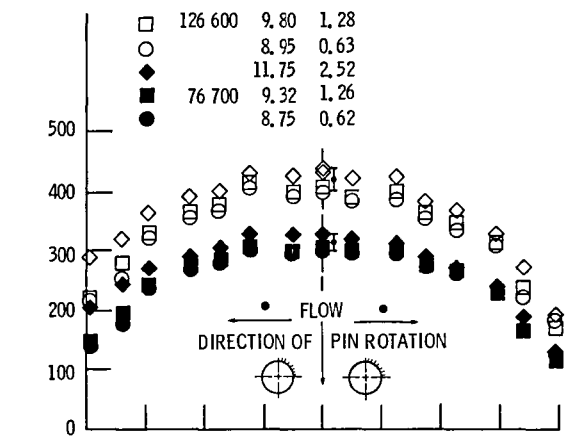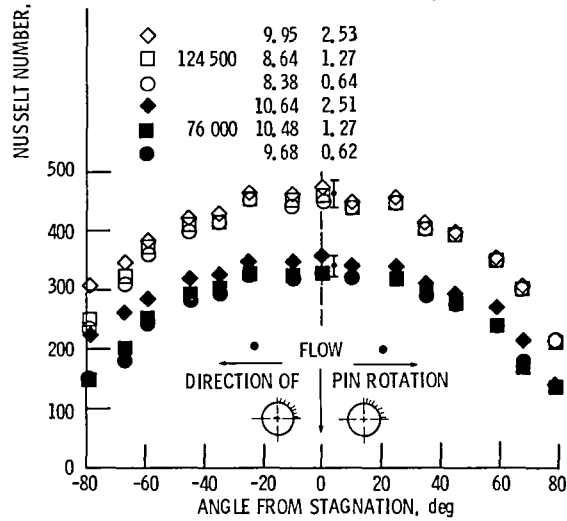
(a) 1.59 mm Pins and 10 mesh grid.

(b) 1.59 mm Pins and 3 mesh grid.

Figure 9. – Effect rotor pin wakes on spanwise average circumferential heat transfer.

□	126 600	9. 80 1. 28
○		8. 95 0. 63
◆		11. 75 2. 52
■	76 700	9. 32 1. 26
●		8. 75 0. 62

FLOW

DIRECTION OF | PIN ROTATION

(c) 3. 18 mm Pins and 10 mesh grid.

◇		9. 95 2. 53
□	124 500	8. 64 1. 27
○		8. 38 0. 64
◆		10. 64 2. 51
■	76 000	10. 48 1. 27
●		9. 68 0. 62

FLOW

DIRECTION OF | PIN ROTATION

ANGLE FROM STAGNATION, deg

NUSSELT NUMBER, Nu

(d) 3. 18 mm Pins and 3 mesh grid.
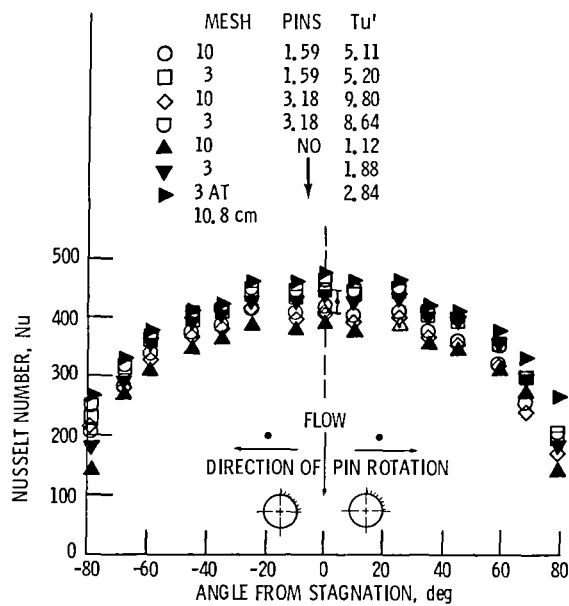
Figure 9. - Concluded.

Figure 10. - Effects of various types of unsteadiness on the circumferential distribution of heat transfer.
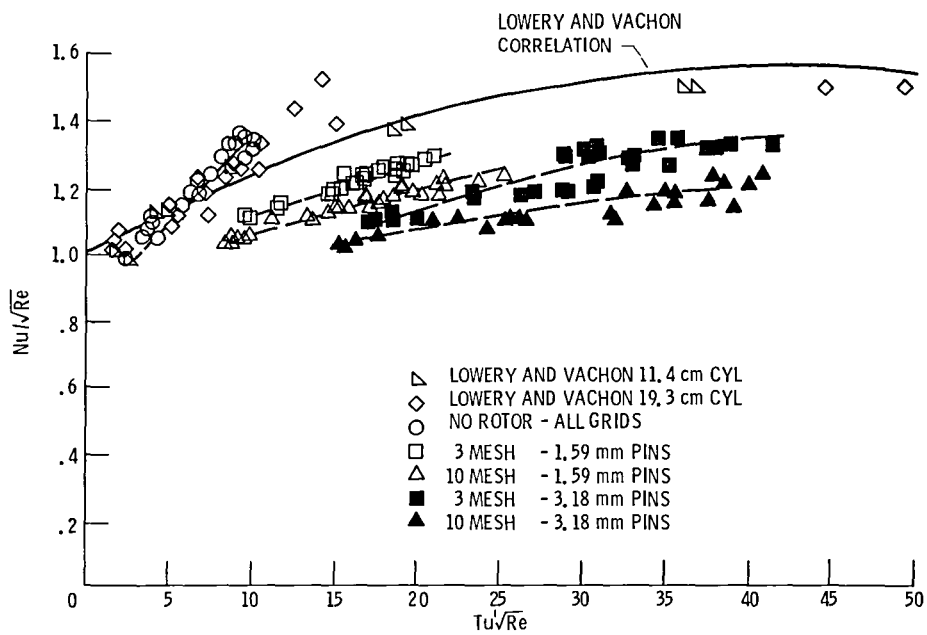

Figure 11. - Comparison of rotor wake stagnation heat transfer data to frequently used correlation.
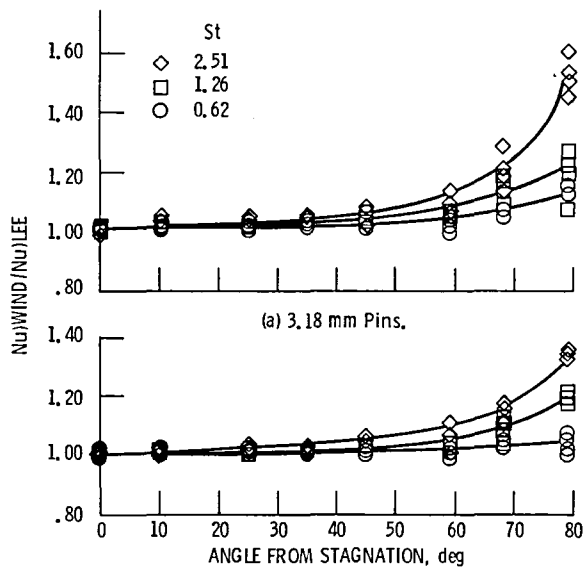
Figure 12. - Heat transfer distribution asymmetry resulting from wake size and rotational speed.

1. Report No. NASA TM-87234	2. Government Accession No.	3. Recipient's Catalog No.
4. Title and Subtitle Effect of a Rotor Wake on the Local Heat Transfer on the Forward Half of a Circular Cylinder		5. Report Date March 1986
		6. Performing Organization Code 505-31-04
7. Author(s) Kim A. Morehouse and Robert J. Simoneau		8. Performing Organization Report No. E-2751
		10. Work Unit No.
9. Performing Organization Name and Address National Aeronautics and Space Administration Lewis Research Center Cleveland, Ohio 44135		11. Contract or Grant No.
		13. Type of Report and Period Covered Technical Memorandum
12. Sponsoring Agency Name and Address National Aeronautics and Space Administration Washington, D.C. 20546		14. Sponsoring Agency Code

15. Supplementary Notes

16. Abstract

An experiment has been developed to simulate the wake dynamics of a turbine rotor-stator combination. The experiment consisted of a spoked wheel rotating in annular flow, generating simulated rotor wakes. The wakes impinged on a simulated stator, composed of a circular cylinder with a splitter plate behind it. The test rig properly simulated the wake shapes and velocity dynamics of a rotating turbine stage. The focus of the research was spanwise averaged circumferentially local heat transfer in the circular cylindrical leading edge region of a turbine airfoil. The range of Reynolds number based on the stator cylinder diameter was 35 000 to 175 000. The reduced blade passing frequencies, or Strouhal numbers, also based on the stator cylinder diameter, ranged from 0.63 to 2.50. The wakes were generated by two different sets of circular cylindrical bars, 1.59 and 3.18 mm in diameter. The rotor could be rotated either clockwise or counterclockwise, causing the wakes to impinge on either the leeward or the windward side of the heated cylinder. In addition, grid turbulence was introduced upstream yielding freestream turbulence of 1.0 to 2.5 percent at the stator location. The data presented in this paper, therefore, represent an extensive body of local heat transfer coefficients, which can be used to develop models in the very important leading edge region of a turbine airfoil. The wakes produced only a modest increase in heat transfer over the baseline no-rotor data. The data in the presence of the rotor wakes showed an asymmetry from the leeward to the windward side. Windward-side levels of from 30 to 40 percent higher than corresponding leeward-side levels were not uncommon, particularly at the combination of high Strouhal number and larger wake generating pins. The stagnation gauge data were examined against the $Tu\sqrt{Re}$ parameter over a wide range from 8 to 40, and found not to be fully correlated by this often used parameter. There were distinct trends with both free-stream turbulence level and wake-generating bar diameter. The results strongly indicate a need to separate the wake influence from turbulence effects.

17. Key Words (Suggested by Author(s)) Rotor wake; Heat transfer; Cylinder	18. Distribution Statement Unclassified - unlimited STAR Category 34
19. Security Classif. (of this report) Unclassified	20. Security Classif. (of this page) Unclassified	21. No. of pages	22. Price*

End of Document